analytical chemistry

Article

pubs.acs.org/ac

Catalytic Hairpin Assembly-Programmed Porphyrin–DNA Complex as Photoelectrochemical Initiator for DNA Biosensing

Yang Zang, Jianping Lei,* Pinghua Ling, and Huangxian Ju

State Key Laboratory of Analytical Chemistry for Life Science, School of Chemistry and Chemical Engineering, Nanjing University, Nanjing 210093, P. R. China

ABSTRACT: A catalytic hairpin assembly (CHA)-programmed porphyrin–DNA complex was designed to trigger the chemiluminescence as photoelectrochemical initiator for DNA sensing. First, the programmed double strand DNA (dsDNA) was formed using two hairpin DNAs as assembly components via target-assisted CHA reaction, and then immobilized on a capture DNA/CdS quantum dots modified electrode. The porphyrin (FeTMPyP) was conveniently assembled on a dsDNA scaffold via the groove interaction. The FeTMPyP@dsDNA complex possessed high catalytic activity toward luminol oxidation to generate the desirable chemiluminescence with high stability under various temperature and alkaline conditions. By integrating the signal amplification capacity of CHA and in situ FeTMPyP-mediated chemiluminescence as excitation light, an amplified photoelectrochemical sensing strategy is proposed for DNA detection. Under optimized conditions, the biosensor shows a wide linear range from 5 to 10000 fM with a detection limit of 2.2 fM. Moreover, the developed photoelectrochemical device exhibits excellent selectivity, high stability, and acceptable fabrication reproducibility. The CHA-programmed porphyrin–DNA strategy not only extends the applications of photoelectrochemistry, but also presents a novel methodology in bioanalysis.

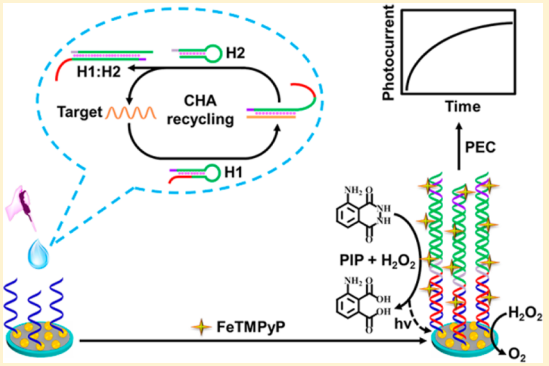

Trace DNA sensing is of significant importance to the detection of many biological markers of disease and has been widely applied in clinical diagnosis and gene therapy.[1−3] Several techniques, such as electrochemiluminescence,[4] electrochemistry,[5,6] photoelectrochemistry (PEC),[7,8] fluorescence,[9] and colorimetry,[10] have been applied for quantitative analysis of DNA. In particular, photoelectrochemical bioassay has offered various elegant routes for biological recognition events due to its low background signal and desirable sensitivity.[11−15] For example, a series of photoelectrochemical sensing strategies based on the steric hindrance, resonance energy transfer, and consumption/generation of coreactant were developed for the detection of DNA, protein, and metal ions.[16−21] However, the conventional photoelectrochemical measurements utilize the physical light source as excitation source, making the instruments and detection process complicated. Meanwhile, various monochromators are needed to excite different photoelectroactive materials, which is unfavorable for the miniaturization of sensing devices.[22] Therefore, searching for a suitable substitute for physical light source to excite photoelectrochemical active materials is highly deserved in practice.

Chemiluminescence (CL), in which chemical reactions are utilized to excite molecules or atoms to bright light emission, has attracted considerable interest.[23] Among them, the enzyme-based oxidation of luminol with H_2O_2 is one primary CL reaction, which can be used to construct a photoelectrochemical biosensor.[24] For example, a sensitive photoelectrochemical analytical protocol with excellent photovoltaic transfer efficiency was developed for CEA detection via horseradish peroxidase (HRP)-triggered CL of luminol-H_2O_2.[25] Unfortunately, the catalytic activity of HRP can be largely decreased under high temperature and alkaline conditions compared to organometallic catalysts. To solve this problem, several mimicking enzymes have been applied in bioanalysis because of their peroxidase-like activity and excellent stability in broad conditions.[26] It has been reported that iron(III) *meso*-tetrakis(*N*-methylpyridinum-4-yl)porphyrin (FeTMPyP) can intercalate into the grooves of double strand DNA (dsDNA), which can maintain its catalytic activity resulting from the protection of the dsDNA scaffold.[27] Thus, based on the interaction of FeTMPyP and dsDNA, a novel mimic enzyme as an photoelectrochemical initiator can be designed for DNA detection.

To further improve the sensitivity of DNA sensing, several signal amplification strategies, such as polymerase chain reaction,[28] rolling circle amplification,[29] and nicking endonuclease-based signal amplification,[30] have been employed to determine biorecognition events. However, the amplified strategies that involved natural enzymes are expensive and need special reaction conditions. For example, polymerase and nicking endonuclease are required in an integrated method of rolling circle amplification and nicking endonuclease-assisted nanoparticle amplification for colorimetric DNA detection.[31]

Received: March 6, 2015
Accepted: April 22, 2015
Published: April 22, 2015

DOI: 10.1021/acs.analchem.5b00888
Anal. Chem. 2015, 87, 5430−5436

Scheme 1. Schematic Illustration of CHA Amplification and FeTMPyP-Mediated Chemiluminescence as Excitation Light for Photoelectrochemical DNA Sensing

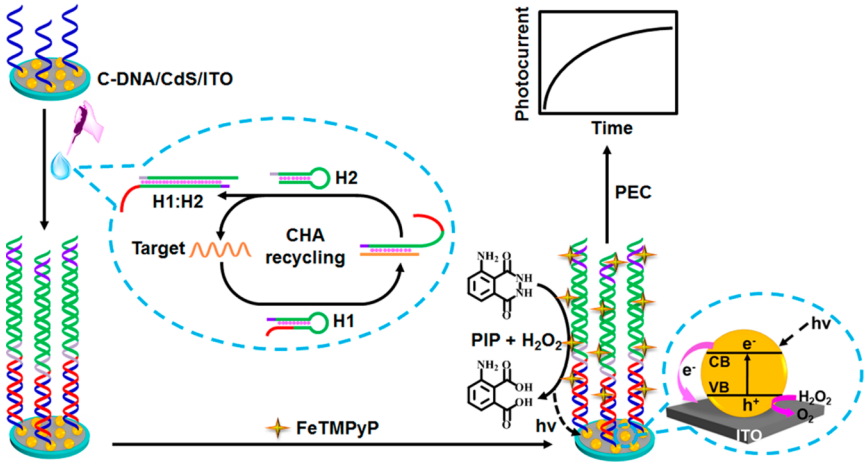

Fortunately, catalytic hairpin assembly (CHA), as an enzyme-free signal amplification technique with negligible background, has been engineered to initiate hundreds-fold catalytic amplification reactions.[32,33] Owing to the programmability, the CHA-based devices may lead to concomitant improvements in convenience and sensitivity.[34] Moreover, a CHA circuit can be used for a specific signal transducer to integrate with other optical or electrochemical techniques.[35−37] However, to date, there has been no report on the CHA-amplified photoelectrochemical biosensor for sensitive DNA detection.

In the present work, we exploited the advantages of CHA and FeTMPyP-mediated chemiluminescence to design an enzyme-free amplified photoelectrochemical DNA sensing strategy (Scheme 1). In the presence of target DNA (tDNA), the CHA routine can be initiated to form a H1:tDNA intermediate, and then catalyzes the dynamic assembly of H1 and H2 to product H1:H2 duplex accompanying the release of tDNA. Meanwhile, the dissociated tDNA can further trigger the hybridization of additional pairs of H1 and H2, promoting the CHA recycling assembly. After incubation with capture DNA (C-DNA), the resulting dsDNA can interact with FeTMPyP to form FeTMPyP@H1:H2:C-DNA on a CdS quantum dots (QDs) modified electrode, which can in situ catalyze the oxidation of luminol to generate chemiluminescence, leading to the significant enhancement of the photocurrent response. On the basis of CHA-based signal amplification and in situ generation of chemiluminescence as excitation light, a sensitive photoelectrochemical DNA biosensor is achieved with desirable selectivity and detection limit down to femtomolar level, showing the potential applicability in bioanalysis and molecular diagnosis.

EXPERIMENTAL SECTION

Materials and Reagents. Indium tin oxide (ITO) electrode was purchased from Zhuhai Kaivo Electronic Components Co. Ltd. (China). Cadmium chloride ($CdCl_2$), thioglycolic acid (TGA), hemin (≥98%), luminol (≥97%), *p*-iodophenol (PIP) (99%), monoethanolamine (MEA), 1-ethyl-3-(3-(dimethylamino)propyl)carbodiimide (EDC), *N*-hydroxysuccinimide (NHS) and horseradish peroxidase were purchased from Sigma-Aldrich. $Na_2S{\cdot}9H_2O$ was obtained from Shanghai Lingfeng Chemical Reagent Co. Ltd. FeTMPyP was a gift from Kanazawa University (Japan). All aqueous solutions were prepared using ultrapure water from a Millipore water purification system (≥18 MΩ, Milli-Q, Millipore). The washing buffer was 20 mM Tris-HCl of pH 7.5 containing 300 mM NaCl. The catalyzed hairpin assembly reaction was performed in 20 mM Tris-HCl of pH 7.5 containing 100 mM NaCl and 5 mM KCl. Twenty mM Tris-HCl of pH 7.5 containing 1 mM MEA was used as blocking solution. All the oligonucleotides used in this work were synthesized and purified by Sangon Biological Engineering Technology & Co. Ltd. (Shanghai, China) and their sequences are summarized below:

Target DNA: 5′-CGACATCTAACCTAGCTCACTGAC-3′

Capture DNA: 5′-NH_2-$(CH_2)_6$-TGACAAGGGCTAGGTT-3′

FITC-labeled capture DNA: 5′-FITC-TGACAAGGGCTAGGTT-3′

Hairpin DNA 1 (H1): 5′-GTCAGTGAGCTAGGTTAGATGTCGCCATGTGTAGACGACATCTAACCTAGCCCTTGTCA-3′

Hairpin DNA 2 (H2): 5′-AGATGTCGTCTACACATGGCGACATCTAACCTAGCCCATGTGTAGA-3′

Single-base mismatched DNA (smDNA): 5′-CGACATCTAACTTAGCTCACTGAC-3′

Three-base mismatched DNA (tmDNA): 5′-CGACACCTAACTTAGCTTACTGAC-3′

S1:5′-GCTAGGTTAGATGTCGCCATGTGTAGACGACATCT-3′

S2:5′-AGATGTCGTCTACACATGGCGACATCTAACCTAGC-3′

G-quadruplex: 5′-GGGTTGGGCGGGATGGG-3′

Apparatus. Transmission electron micrograph (TEM) was performed using a JEM-2100 microscope (JEOL, Japan). UV−vis absorption spectra were obtained using a UV-3600 UV−vis−near-infrared spectrophotometer (Shimadzu Co. Kyoto, Japan). The CL signals were recorded on an IFFM-E Luminescent Analyzer (Remax, China). Dynamic light scattering (DLS) measurement was performed by BI-200 SM light scattering apparatus (Brookhaven Instruments Co. USA) equipped with a digital correlator at 640 nm. The X-ray photoelectron spectrum (XPS) was recorded on an ESCALAB 250 spectrometer (Thermo-VG Scientic Co. USA) with an ultrahigh vacuum generator. Photoelectrochemical detections were carried out with a home-built photoelectrochemical

DOI: 10.1021/acs.analchem.5b00888
Anal. Chem. 2015, 87, 5430−5436

system. Gel electrophoresis analysis was performed on the DYCP-31 BN electrophoresis analyzer (Liuyi Instrument Company, China) and imaged on the Biorad ChemDoc XRS (USA). Electrochemical impedance spectroscopy (EIS) was conducted using a PGSTAT30/FRA2 system (Autolab, The Netherlands) in 0.1 M Na_2SO_4 solution containing 5 mM $K_4[Fe(CN)_6]/K_3[Fe(CN)_6]$ (1:1) mixture as the negatively charged redox probe from 0.1 Hz to 100 kHz with a signal amplitude of 5 mV and the applied potential of 0.180 V. All experiments were performed at room temperature using a conventional three-electrode system with a modified ITO electrode (4 mm in diameter) as the working, platinum electrode as the auxiliary, and saturated calomel as the reference electrodes.

Gel Electrophoresis. The 10% native polyacrylamide gel electrophoresis (PAGE) was prepared by using 1 × Tris-borate-EDTA (TBE) buffer. The loading sample was mixed with 7 μL of DNA sample, 1.5 μL 6 × loading buffer, and 1.5 μL UltraPowerTM dye, and kept for 3 min so that the dye can integrate with DNA completely. The gel electrophoresis was run at 90 V for 90 min in 1 × TBE buffer. The resulting board was illuminated with UV light and photographed with a Molecular Imager Gel Doc XR.

Synthesis of TGA-Capped CdS QDs. CdS QDs were synthesized according to the previous report.[21] Typically, 250 μL of TGA was injected into 50 mL of 0.01 M $CdCl_2$ aqueous solution in N_2 atmosphere. After being adjusted to pH 11 with 1.0 M NaOH, 5.0 mL of 0.1 M Na_2S aqueous solution was injected, and refluxed for 4 h to obtain TGA-capped water-soluble CdS QDs. Before usage, this QDs solution was sedimentated with isopropanol and collected by centrifugation, and then the colloidal precipitate was dissolved with an equivalent amount of deionized water.

Construction of Photoelectrochemical Biosensor. Prior to sensor fabrication, the ITO electrode was immersed in boiling 2-propanol solution containing 1.0 M NaOH for 15 min, followed by ultrasonic cleaning with 10% H_2O_2, acetone and deionized water. After washed with deionized water and blow-dried with nitrogen, 10 μL of CdS QDs was immobilized on ITO electrode surface via physical adsorption and dried at room temperature. The carboxylic group on modified electrode surface was activated using 10 mM PBS buffer of pH 5.3 containing 10 mM EDC and 20 mM NHS for 1 h at room temperature. Subsequently, the activated electrode was washed with PBS buffer, and 20 μL of 1.5 μM C-DNA was dropped onto its surface to incubate at 4 °C overnight. After incubation, the electrode was rinsed three times to remove the non-conjugated DNA. The resulting electrode was blocked with 20 μL of 1 mM MEA for 2 h at 4 °C and rinsed with washing buffer thoroughly. Finally, the prepared biosensor was kept in 4 °C for subsequent experiments.

Analytical Procedure. Before experiments, H1 and H2 were separately annealed at 90 °C for 5 min followed by slowly decreasing to room temperature. To proceed the CHA reaction, the mixture containing 200 nM H1, 300 nM H2 and different concentrations of target DNA was incubated at 37.1 °C for 1 h. Then, 20 μL of the resulting solution was applied to electrode surface to incubate at 37.1 °C for another 2 h. Subsequently, the modified electrode was incubated with 20 μL of 5 μM FeTMPyP for 1 h. The modified electrode was washed with Tris-HCl buffer and dried under N_2 atmosphere after each modification step. Finally, the photoelectrochemical signal was recorded in 0.1 M Tris-HCl buffer of pH 9.0 containing 25 mM H_2O_2, 0.6 mM PIP and 0.6 mM luminol at a constant potential of +0.2 V for DNA detection.

RESULTS AND DISCUSSION

Characterization of CdS QDs. To characterize the morphology of CdS ODs, a DLS spectrum and TEM image were obtained in Figure 1. As shown in Figure 1A, the mean

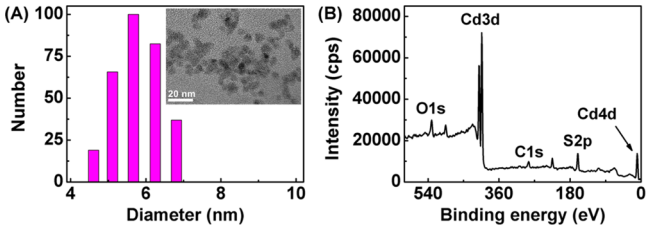

Figure 1. (A) Hydrodynamic size distribution measured by DLS and (B) XPS spectrum of CdS QDs. Inset of panel A is TEM image of CdS QDs.

hydrodynamic diameter of TGA-capped CdS QDs was 5.9 nm. Meanwhile, the TEM image showed the obtained CdS QDs were quasi-spherical nanoparticles with an average size of 5.0 nm (inset in Figure 1A), which was identical with the DLS result. The surface chemical composition of QDs was characterized by XPS (Figure 1B). The XPS of Cd 3d showed two strong peaks at 403.8 and 410.9 eV, corresponding to Cd $3d_{5/2}$ and Cd $3d_{3/2}$ levels of QDs, respectively.[25] Besides, carbon (284.4 eV of C 1s), oxygen (531.8 eV of O 1s), and sulfur (161.1 eV of S 2p) were also observed as a result of surface modification of TGA, which was beneficial to the covalent assembly of capture DNA.

Stability of FeTMPyP@dsDNA Complex. The stability of mimicking enzyme was an important parameter for the detection performance of our designed biosensor. The effects of temperature and alkaline conditions were evaluated on catalytic activity of HRP, hemin/G-quadruplex DNAzyme, and FeTMPyP@dsDNA in the luminol−H_2O_2−PIP system. As shown in Figure 2A, the FeTMPyP@dsDNA complex as a mimic enzyme could maintain 85% of its initial catalytic activity even at 60 °C, which was much higher than those of 8% and 65% for HRP and hemin/G-quadruplex DNAzyme, respectively, indicating the excellent thermostability of FeTMPyP@dsDNA. Moreover, after incubation at pH 9.0 buffer for 1 h, the catalytic activity of FeTMPyP@dsDNA and hemin/G-quadruplex DNAzyme had almost unchanged while HRP lost 55% of its catalytic performance (Figure 2B), which demonstrated that FeTMPyP@dsDNA was more stable than HRP at high pH value. Thus, the proposed FeTMPyP@dsDNA as a mimic catalyst displayed favorable stability under high temperature and high pH, showing great applications in broad fields.

To investigate the validity of a proposed biosensor, the chemiluminescence spectrum of the FeTMPyP@dsDNA complex and the UV−vis absorption spectrum of CdS QDs were obtained (Figure 2C). The chemiluminescence generated by catalytic oxidation of FeTMPyP@dsDNA in luminol−H_2O_2−PIP solution showed a maximum emission peak at *ca.* 426 nm (curve a), whereas CdS QDs as a photoactive substrate have a broad absorption range below 500 nm (curve b). Obviously, the CL spectrum generated by luminol oxidation has a large spectral overlap with the absorption spectrum of CdS QDs, suggesting that the light generated by chemilumi-

DOI: 10.1021/acs.analchem.5b00888
Anal. Chem. 2015, 87, 5430−5436

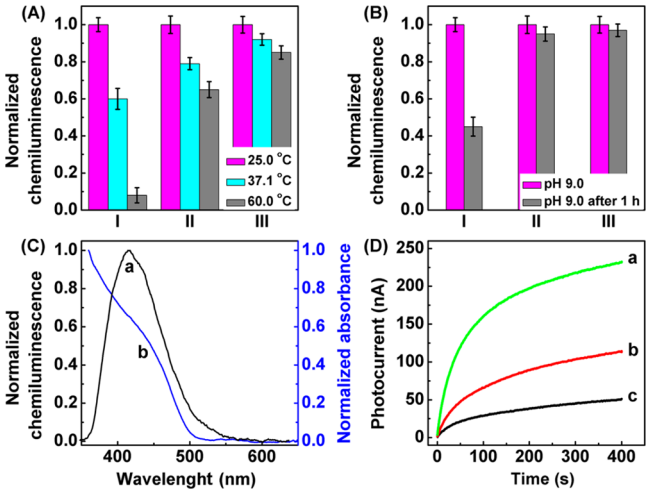

Figure 2. Effects of (A) temperature for 0.5 h, and (B) alkaline conditions for 1 h on chemiluminescence catalyzed by HRP (I), hemin/G-quadruplex DNAzyme (II), and FeTMPyP@dsDNA complex (III) in the luminol–H_2O_2–PIP system. (C) Spectral overlap between the chemiluminescence spectrum of luminol (a) and the UV–vis absorption spectrum of CdS QDs (b). (D) Photocurrent response of FeTMPyP@H1:H2:C-DNA/CdS (a, b) and H1:H2:C-DNA/CdS (c) modified ITO electrode in 0.1 M Tris-HCl buffer of pH 9.0 containing 25 mM H_2O_2 and 0.6 mM luminol with (a, c) and without (b) 0.6 mM PIP.

nescence could lead to the excitation of QDs and the generation of electron–hole pairs. The ejection of conduction-band (CB) electrons to ITO electrode and the concomitant scavenging of valence-band (VB) holes by the oxidation of H_2O_2 resulted in a stable anodic photocurrent (Scheme 1). To further verify the PEC response of the biosensor, Figure 2D showed the photocurrent response of modified electrodes in different electrolytes. In the luminol–H_2O_2–PIP solution, the photocurrent of DNA biosensor (curve a) enhanced 4.3 times than that of H1:H2:C-DNA/CdS modified ITO electrode (curve c), demonstrating that FeTMPyP@dsDNA as a mimic enzyme was suitable for CL-stimulated generation of photocurrents. However, the photocurrent of the proposed biosensor was only 115 nA in the absence of PIP (curve b), which was attributed to the concept that PIP as a CL intensifier could significantly enhance the photocurrent response. Overall, using CL-stimulated generation of photocurrents could be utilized to detect DNA analyte without external irradiation.

Feasibility of Photoelectrochemical Biosensor. To evaluate the feasibility of CHA, the gel electrophoresis analysis of different DNAs was recorded (Figure 3A). Although H1 (lane a) and H2 (lane b) contained complementary sequences, their mixture did not show the change of band positions after incubation for 3 h (lane e), indicating no hybridization occurred between the two hairpin DNAs. Similarly, no apparent change was observed in the mixture of H1 and C-DNA (lane f). When target DNA was added into the mixture of H1 and H2, a new band corresponding to H1:H2 duplex appeared at a short electrophoresis distance, while the bands corresponding to H1 and H2 almost completely disappeared (lane g), which could be attributed to the successful dynamic assembly catalyzed by target DNA. What's more, after adding C-DNA into the mixture of H1, H2, and target DNA, a clear band at a shorter

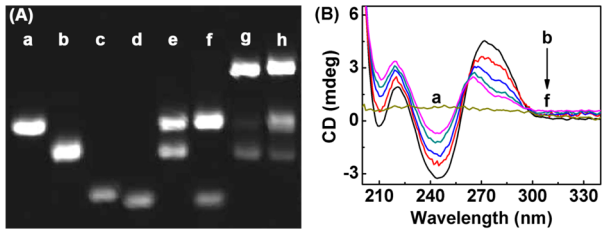

Figure 3. (A) Gel electrophoresis images of 2 μM H1 (a), H2 (b), target DNA (c), C-DNA (d), mixture of 2 μM H1 and 2 μM H2 (e), mixture of 2 μM H1 and 2 μM C-DNA (f), (e) incubation with 20 nM target DNA (g), (g) incubation with 2 μM C-DNA (h). (B) CD spectra of 25 μM FeTMPyP (a), H1:H2:C-DNA duplex (b), (b) + 25 μM FeTMPyP (c), (b) + 50 μM FeTMPyP (d), (b) + 75 μM FeTMPyP (e), (b) + 100 μM FeTMPyP (f).

electrophoresis distance was observed (lane h), confirming the formation of H1:H2:C-DNA duplex.

Besides, CD spectra were investigated for verifying the formation of FeTMPyP@dsDNA complex (Figure 3B). Free FeTMPyP did not show any detectable CD absorption (curve a), while the H1:H2:C-DNA exhibited two typical CD bands of the right-handed B-helix at 250 and 272 nm (curve b).[38] When FeTMPyP was added into H1:H2:C-DNA solution, the CD bands of H1:H2:C-DNA reduced, demonstrating that FeTMPyP@H1:H2:C-DNA complex had been programmed successfully due to the groove interaction between H1:H2:C-DNA and FeTMPyP. Moreover, with the FeTMPyP concentration up to 100 μM in H1:H2:C-DNA solution (curve f), only small CD absorption was observed, which indicated that most DNA-binding sites were occupied by FeTMPyP. Thus, dsDNA as an efficient carrier was enough for loading of FeTMPyP to stimulate luminol-based chemiluminescence.

EIS Characterization of the Biosensor. As a powerful tool to analyze the interface properties of electrodes, EIS was employed to investigate the stepwise assembly process of photoelectrochemical sensing platform. Figure 4 showed the

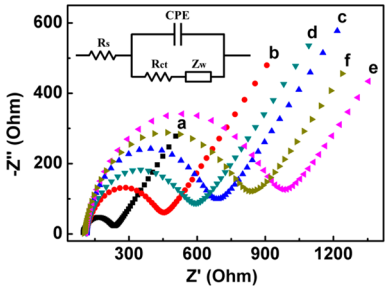

Figure 4. EIS spectra of bare ITO (a), CdS (b), C-DNA/CdS (c), (c) blocked by MEA (d), H1:H2:C-DNA/CdS (e), and FeTMPyP@H1:H2:C-DNA/CdS modified ITO electrode (f) in 0.1 M Na_2SO_4 solution containing a 5 mM $K_4[Fe(CN)_6]/K_3[Fe(CN)_6]$ (1:1) mixture. Inset: the electrical equivalent circuit applied to fit the impedance data; R_s, Z_w, R_{ct}, and CPE represent the Ohmic resistance of the electrolyte, Warburg impedance, charge-transfer resistance, and constant phase angle element, respectively.

impedance spectra of modified electrodes formed in different construction steps and its corresponding equivalent circuit (inset in Figure 4). Compared to 133.5 Ω for ITO electrode (curve a), the impedance spectrum of CdS modified ITO electrode showed a higher charge-transfer resistance (R_{ct}) of 318.5 Ω (curve b) owing to the low conductivity of QDs. With

DOI: 10.1021/acs.analchem.5b00888
Anal. Chem. 2015, 87, 5430–5436

the C-DNA assembled on CdS/ITO electrode, the value of R_{ct} increased significantly to 530.7 Ω (curve c). After blocked by MEA (curve d), R_{ct} value declined to 450.7 Ω because of the electrostatic interaction between negatively charged redox probe and the positively charged MEA. Besides, when the hybridization of C-DNA and H1:H2 duplex occurred, R_{ct} value of H1:H2:C-DNA/CdS modified ITO electrode increased significantly to 817.7 Ω owing to steric hindrance effect (curve e), and then decreased to 688.0 Ω after intercalation positively charged FeTMPyP (curve f), suggesting the proposed biosensor was constructed as expected, providing a sensitive sensing platform for DNA detection.

Optimization of Detection Conditions. The photoelectrochemical performance of the biosensor largely depended on H_2O_2 concentration, capture DNA concentration, FeTMPyP concentration, and incubation time of CHA (Figure 5). As

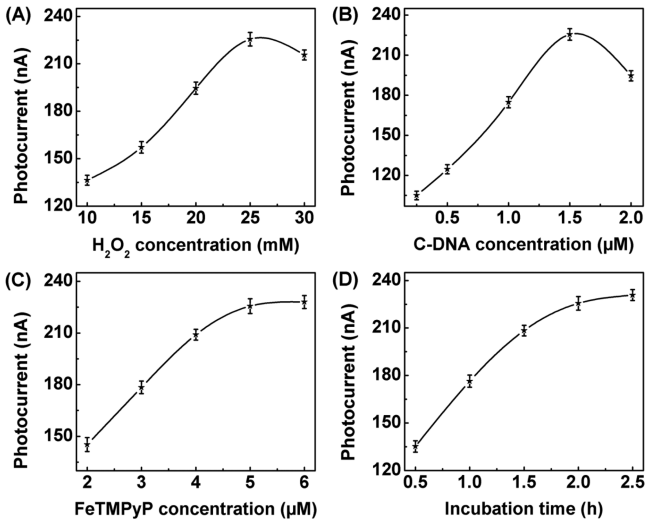

Figure 5. Effects of (A) H_2O_2 concentration, (B) capture DNA concentration, (C) FeTMPyP concentration, and (D) incubation time of CHA reaction on the photocurrent response of the biosensor.

displayed in Figure 5A, the photocurrent response generated by luminol-H_2O_2 reaction was investigated by changing the content of H_2O_2 in the electrolyte solution. The photocurrent increased with the increasing of H_2O_2 concentration up to 25 mM and then slightly decreased with further addition of H_2O_2 because of H_2O_2-mediated oxidation of the surface of CdS QDs.[39] Thus, 25 mM H_2O_2 was employed for the next experiments. Similarly, the increasing concentration of capture DNA up to 1.5 μM could enhance the photocurrent response, and further increasing of C-DNA concentration led to a sharp decrease of photocurrent (Figure 5B), indicating that the efficiency of DNA hybridization became lower at high concentration of C-DNA owing to its steric hindrance. Thus, 1.5 μM C-DNA was chosen for the preparation of biosensor.

The amounts of FeTMPyP intercalated into dsDNA grooves affected greatly the sensitivity of the biosensor (Figure 5C). As the concentration of FeTMPyP increased, the photocurrent increased significantly because of the enhancement of chemiluminescence, and reached the plateau at 5 μM, indicating the saturated binding of FeTMPyP to dsDNA. Thus, 5 μM was selected for following photoelectrochemical measurements. In addition, the incubation time of modified electrode with the reaction mixture of H1, H2 and target DNA was further optimized (Figure 5D). With the incubation time increased, more H1:H2 duplex was immobilized by C-DNA followed by the formation of FeTMPyP@dsDNA, thus the photocurrent intensity increased and trended to level off at 2 h, which was chosen as the optimal reaction condition.

Analytical Performance of Photoelectrochemical Biosensor. On the basis of CHA and CL-based signal amplification, a novel photoelectrochemical sensing strategy for DNA detection was proposed via the successful fabrication of FeTMPyP@dsDNA complex. Figure 6A exhibits the

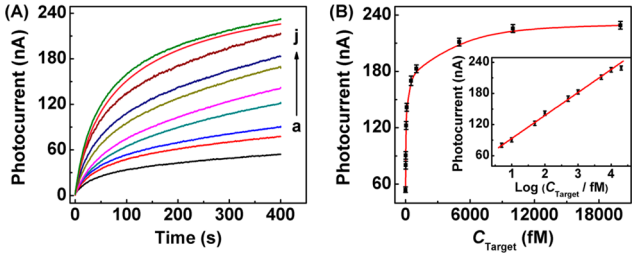

Figure 6. (A) Photocurrent response of the proposed sensor at 0, 5, 10, 50, 100, 500, 1000, 5000, 10000, and 20000 fM target DNA (from a to j). (B) Plot of photocurrent intensity versus DNA concentration. Inset: calibration curve. The photocurrent intensities were recorded at 400 s.

photocurrent response measured at different concentrations of DNA. In the absence of target DNA, a low photocurrent was obtained due to the lack of excitation light. As the concentration of target DNA increased, the photocurrent intensity increased gradually, indicating the formation of FeTMPyP@dsDNA could produce chemiluminescence and facilitate the excitation of CdS QDs.

The photocurrent intensity of designed biosensor was directly related to target DNA concentration. The calibration plot of photocurrent intensity versus the logarithm of target DNA concentration from 5 to 10000 fM showed a good linearity (Figure 6B). The linear range was wider than that of photoelectrochemistry based on isothermal circular strand-displacement polymerization reaction (0.1−8.0 nM),[40] exonuclease III-assisted electrochemical (20−300 pM)[41] and chemiluminescenct methods (0.01−1.0 pM).[42] The regression equation was I (nA) = 48.72 + 44.38 log C (fM) with a correlation coefficient of 0.997, where I is the photocurrent of the biosensor in the presence of target DNA, and C is the concentration of target DNA. The limit of detection was estimated to be 2.2 fM at 3σ, which was much lower than 20 fM of exonuclease-assisted fluorescence method and 50 pM of hybridization chain reaction-based colorimetric method.[43,44] Apparently, the proposed photoelectrochemical biosensor had desirable linear range and high sensitivity because of signal amplification of CHA and excellent catalytic activity of FeTMPyP@dsDNA complex.

Selectivity and Stability of Photoelectrochemical Biosensor. To evaluate the selectivity of the designed biosensor, the effect of different DNA sequences including target DNA, smDNA, and tmDNA on photocurrent changes was investigated (Figure 7). The ΔI of target DNA was 5.6 and 8.7 times higher than that of smDNA and tmDNA, respectively. These results demonstrated that the biosensor had excellent selectivity for target DNA against base mismatched sequences. Moreover, the assay precision of biosensor was also measured by five independent electrodes. The relative standard deviation of photocurrent response was 4.3% for 10 pM target DNA,

DOI: 10.1021/acs.analchem.5b00888
Anal. Chem. 2015, 87, 5430−5436

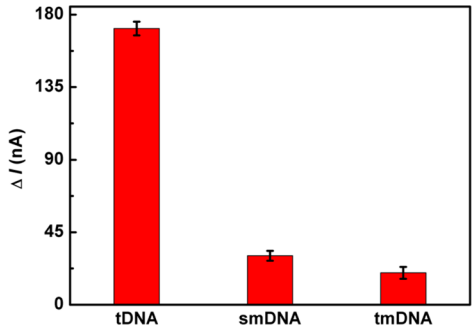

Figure 7. Photocurrent changes of the designed biosensor at 10 pM of target DNA, smDNA, and tmDNA. $\Delta I = I - I_0$, where I and I_0 are the photocurrents of biosensor with and without target DNA, respectively.

giving acceptable precision and fabrication reproducibility. The long-time stability of the constructed biosensor was examined, and the biosensor was kept in dark condition at 4 °C when it was not in use. The photocurrent intensity of the biosensor did not show an obvious change after storage for 10 days. Thus, this biosensor has acceptable longtime stability.

CONCLUSION

In summary, we have successfully constructed an enzyme-free photoelectrochemical biosensor for ultrasensitive quantitative detection of DNA at the femtomolar level based on target-catalyzed hairpin assembly and FeTMPyP-mediated chemiluminescence. This signal amplification strategy relies on the CHA-programmed duplex on the modified electrode surface and the intercalation of massive FeTMPyP into the dsDNA grooves. The formation of FeTMPyP@dsDNA allows FeTMPyP to maintain efficient catalytic activity due to the inhibition of molecular aggregation. With the catalytic oxidation of FeTMPyP in luminol−H_2O_2−PIP solution, chemiluminescence was generated as excitation light and subsequently facilitated the substantial enhancement of photocurrent signal. By integration of the signal amplification of CHA, low background of PEC, and low cost of CL, the proposed photoelectrochemical DNA biosensor shows high sensitivity, wide linear range, and excellent selectivity, which was comparable to or even better than most amplified DNA biosensors. Thus, this designed sensing strategy served as a universal tool can be expanded to detect different target DNA via designing of the corresponding hairpin DNA sequences.

AUTHOR INFORMATION

Corresponding Author

*Phone/Fax: +86-25-83593593. E-mail: jpl@nju.edu.cn.

Notes

The authors declare no competing financial interest.

ACKNOWLEDGMENTS

We gratefully acknowledge the National Natural Science Foundation of China (21375060, 21135002, 21121091) and Priority development areas of the National Research Foundation for the Doctoral Program of Higher Education of China (20130091130005).

REFERENCES

(1) Lockhart, D. J.; Winzeler, E. A. *Nature* **2000**, *405*, 827−836.
(2) Lu, C. H.; Wang, F. A.; Willner, I. *J. Am. Chem. Soc.* **2012**, *134*, 10651−10658.
(3) Furst, A.; Landefeld, S.; Hill, M. G.; Barton, J. K. *J. Am. Chem. Soc.* **2013**, *135*, 19099−19102.
(4) Tang, X. F.; Zhao, D.; He, J. C.; Li, F. W.; Peng, J. X.; Zhang, M. N. *Anal. Chem.* **2013**, *85*, 1711−1718.
(5) Cunningham, J. C.; Brenes, N. J.; Crooks, R. M. *Anal. Chem.* **2014**, *86*, 6166−6170.
(6) Eltzov, E.; Cosnier, S.; Marks, R. S. *Expert Rev. Mol. Diagn.* **2011**, *11*, 533−546.
(7) Lu, W.; Jin, Y.; Wang, G.; Chen, D.; Li, J. H. *Biosens. Bioelectron.* **2008**, *23*, 1534−1539.
(8) Zhao, W. W.; Wang, J.; Xu, J. J.; Chen, H. Y. *Chem. Commun.* **2011**, *47*, 10990−10992.
(9) Lei, C. Y.; Huang, Y.; Nie, Z.; Hu, J.; Li, L. J.; Lu, G. Y.; Han, Y. T.; Yao, S. Z. *Angew. Chem., Int. Ed.* **2014**, *53*, 8358−8362.
(10) Ji, H. X.; Dong, H. F.; Yan, F.; Lei, J. P.; Ding, L.; Gao, W. C.; Ju, H. X. *Chem.—Eur. J.* **2011**, *17*, 11344−11349.
(11) Long, Y. T.; Kong, C.; Li, D. W.; Li, Y.; Chowdhury, S.; Tian, H. *Small* **2011**, *7*, 1624−1628.
(12) Grätzel, M. *Nature* **2001**, *414*, 338−344.
(13) Yin, H. S.; Sun, B.; Zhou, Y. L.; Wang, M.; Xu, Z. N.; Fu, Z. L.; Ai, S. Y. *Biosens. Bioelectron.* **2014**, *51*, 103−108.
(14) Haddour, N.; Chauvin, J.; Gondran, C.; Cosnier, S. *J. Am. Chem. Soc.* **2006**, *128*, 9693−9698.
(15) Chen, D.; Zhang, H.; Li, X.; Li, J. H. *Anal. Chem.* **2010**, *82*, 2253−2261.
(16) Zang, Y.; Lei, J. P.; Zhang, L.; Ju, H. X. *Anal. Chem.* **2014**, *86*, 12362−12368.
(17) Haddache, F.; Le Goff, A.; Reuillard, B.; Gorgy, K.; Gondran, C.; Spinelli, N.; Defrancq, E.; Cosnier, S. *Chem.—Eur. J.* **2014**, *20*, 15555−15560.
(18) Yin, H. S.; Wang, M.; Zhou, Y. L.; Zhang, X. Y.; Sun, B.; Wang, G. H.; Ai, S. Y. *Biosens. Bioelectron.* **2014**, *53*, 175−181.
(19) Yao, W. J.; Le Goff, A.; Spinelli, N.; Holzinger, M.; Diao, G. W.; Shan, D.; Defrancq, E.; Cosnier, S. *Biosens. Bioelectron.* **2013**, *42*, 556−562.
(20) Zeng, X. X.; Ma, S. S.; Bao, J. C.; Tu, W. W.; Dai, Z. H. *Anal. Chem.* **2013**, *85*, 11720−11724.
(21) Zang, Y.; Lei, J. P.; Hao, Q.; Ju, H. X. *ACS Appl. Mater. Interfaces* **2014**, *6*, 15991−15997.
(22) Zhang, X. R.; Zhao, Y. Q.; Zhou, H. R.; Qu, B. *Biosens. Bioelectron.* **2011**, *26*, 2737−2741.
(23) Zong, C.; Wu, J.; Wang, C.; Ju, H. X.; Yan, F. *Anal. Chem.* **2012**, *84*, 2410−2415.
(24) Ding, C. F.; Li, H.; Li, X. L.; Zhang, S. S. *Chem. Commun.* **2010**, *46*, 7990−7992.
(25) Tu, W. W.; Wang, W. J.; Lei, J. P.; Deng, S. Y.; Ju, H. X. *Chem. Commun.* **2012**, *48*, 6535−6537.
(26) Xu, J.; Wu, J.; Zong, C.; Ju, H. X.; Yan, F. *Anal. Chem.* **2013**, *85*, 3374−3379.
(27) Li, J.; Lei, J. P.; Wang, Q. B.; Wang, P.; Ju, H. X. *Electrochim. Acta* **2012**, *83*, 73−77.
(28) Qiu, L. P.; Wu, Z. S.; Shen, G. L.; Yu, R. Q. *Anal. Chem.* **2011**, *83*, 3050−3057.
(29) Wang, F.; Lu, C. H.; Liu, X. Q.; Freage, L.; Willner, I. *Anal. Chem.* **2014**, *86*, 1614−1621.
(30) Liu, Z. Y.; Zhang, W.; Zhu, S. Y.; Zhang, L.; Hu, L. Z.; Parveen, S.; Xu, G. B. *Biosens. Bioelectron.* **2011**, *29*, 215−218.
(31) Xu, W.; Xie, X. J.; Li, D. W.; Yang, Z. Q.; Li, T. H.; Liu, X. G. *Small* **2012**, *8*, 1846−1850.
(32) Li, B. L.; Jiang, Y.; Chen, X.; Ellington, A. D. *J. Am. Chem. Soc.* **2012**, *134*, 13918−13921.
(33) Zhuang, J. Y.; Lai, W. Q.; Chen, G. N.; Tang, D. P. *Chem. Commun.* **2014**, *50*, 2935−2938.
(34) Jiang, Y.; Li, B. L.; Milligan, J. N.; Bhadra, S.; Ellington, A. D. *J. Am. Chem. Soc.* **2013**, *135*, 7430−7433.
(35) Li, B. L.; Ellington, A. D.; Chen, X. *Nucleic Acids Res.* **2011**, *39*, e110.

DOI: 10.1021/acs.analchem.5b00888
Anal. Chem. 2015, 87, 5430−5436

(36) Qing, Z. H.; He, X. X.; Huang, J.; Wang, K. M.; Zou, Z.; Qing, T. P.; Mao, Z. G.; Shi, H.; He, D. G. *Anal. Chem.* **2014**, *86*, 4934−4939.
(37) Liu, S. F.; Wang, Y.; Ming, J. J.; Lin, Y.; Cheng, C. B.; Li, F. *Biosens. Bioelectron.* **2013**, *49*, 472−477.
(38) Vorlíčková, M.; Kejnovská, I.; Bednářová, K.; Renčiuk, D.; Kypr, J. *Chirality* **2012**, *24*, 691−698.
(39) Mancini, M. C.; Kairdolf, B. A.; Smith, A. M.; Nie, S. M. *J. Am. Chem. Soc.* **2008**, *130*, 10836−10837.
(40) Zhang, X. R.; Xu, Y. P.; Zhao, Y. Q.; Song, W. L. *Biosens. Bioelectron.* **2013**, *39*, 338−341.
(41) Xuan, F.; Luo, X. T.; Hsing, I. M. *Anal. Chem.* **2012**, *84*, 5216−5220.
(42) Gao, Y.; Li, B. X. *Anal. Chem.* **2014**, *86*, 8881−8887.
(43) Liu, S. F.; Cheng, C. B.; Liu, T.; Wang, L.; Gong, H. W.; Li, F. *Biosens. Bioelectron.* **2015**, *63*, 99−104.
(44) Liu, P.; Yang, X. H.; Sun, S.; Wang, Q.; Wang, K. M.; Huang, J.; Liu, J. B.; He, L. L. *Anal. Chem.* **2013**, *85*, 7689−7695.

DOI: 10.1021/acs.analchem.5b00888
Anal. Chem. 2015, 87, 5430−5436